

SANDIA REPORT

SAND2003-8796

Unlimited Release

Printed December, 2003

Advanced Digital Detectors for Neutron Imaging

F. P. Doty
Engineered Materials Department

Prepared by
Sandia National Laboratories
Albuquerque, New Mexico 87185 and Livermore, California 94550

Sandia is a multiprogram laboratory operated by Sandia Corporation,
a Lockheed Martin Company, for the United States Department of Energy's
National Nuclear Security Administration under Contract DE-AC04-94AL85000.

Approved for public release; further dissemination unlimited.



Sandia National Laboratories

Issued by Sandia National Laboratories, operated for the United States Department of Energy by Sandia Corporation.

NOTICE: This report was prepared as an account of work sponsored by an agency of the United States Government. Neither the United States Government, nor any agency thereof, nor any of their employees, nor any of their contractors, subcontractors, or their employees, make any warranty, express or implied, or assume any legal liability or responsibility for the accuracy, completeness, or usefulness of any information, apparatus, product, or process disclosed, or represent that its use would not infringe privately owned rights. Reference herein to any specific commercial product, process, or service by trade name, trademark, manufacturer, or otherwise, does not necessarily constitute or imply its endorsement, recommendation, or favoring by the United States Government, any agency thereof, or any of their contractors or subcontractors. The views and opinions expressed herein do not necessarily state or reflect those of the United States Government, any agency thereof, or any of their contractors.

Printed in the United States of America. This report has been reproduced directly from the best available copy.

Available to DOE and DOE contractors from
U.S. Department of Energy
Office of Scientific and Technical Information
P.O. Box 62
Oak Ridge, TN 37831

Telephone: (865)576-8401
Facsimile: (865)576-5728
E-Mail: reports@adonis.osti.gov
Online ordering: <http://www.doe.gov/bridge>

Available to the public from
U.S. Department of Commerce
National Technical Information Service
5285 Port Royal Rd
Springfield, VA 22161

Telephone: (800)553-6847
Facsimile: (703)605-6900
E-Mail: orders@ntis.fedworld.gov
Online order: <http://www.ntis.gov/help/ordermethods.asp?loc=7-4-0#online>



SANDIA REPORT
SAND 2003-8796
Unlimited Release
Printed December, 2003

Advanced Digital Detectors for Neutron Imaging

F. P. Doty
Engineered Materials Department
Sandia National Laboratories
P. O. Box 0969
Livermore, CA

Abstract

Neutron interrogation provides unique information valuable for Nonproliferation & Materials Control and other important applications including medicine, airport security, protein crystallography, and corrosion detection. Neutrons probe deep inside massive objects to detect small defects and chemical composition, even through high atomic number materials such as lead. However, current detectors are bulky gas-filled tubes or scintillator/PM tubes, which severely limit many applications. Therefore this project was undertaken to develop new semiconductor radiation detection materials to develop the first direct digital imaging detectors for neutrons. The approach relied on new discovery and characterization of new solid-state sensor materials which convert neutrons directly to electronic signals via reactions $B^{10}(n,\alpha)Li^7$ and $Li^6(n,\alpha)T$.

Acknowledgements

The support of 8700 staff including Richard Olsen for electrical measurements, Doug Chinn for materials science and device fabrication, Dan Morse for operation of the proton microprobe, and Arlyn Antolak for analysis and stimulating discussions is gratefully acknowledged.

Contents

INTRODUCTION	6
EXPERIMENTAL DETAILS	7
Physics of Detector Operation	7
Measurement Circuit	7
RESULTS	8
Survey of Candidate Materials.....	8
Investigation of pyrolytic BN	10
Investigation of Borate Crystals	10
Investigation of polymer composite materials	11
SUMMARY AND CONCLUSION	12
TABLES	
Table 1 Survey of candidate materials.....	8
Table 2 properties of pyrolytic BN	9
FIGURES	
Figure 1 Measurement circuit block diagram	13
Figure 2 SEM micrograph of pBN	14
Figure 3 Response of pBN device to alpha radiation	14
Figure 4 Bias dependence of pBN response	14
Figure 5 Electron and hole Hecht plots for pBN	14
Figure 6 Transient response of pBN with reactor thermal neutrons	15
Figure 7 Pulse distribution of pBN with reactor thermal neutrons.....	16
Figure 8 Pulse distribution of pBN with isotopic alphas	16
Figure 9 Neutron response of alpha barium borate	17
Figure 10 Single-layer gel film of lithium borate hydrate	18
Figure 11 Multi-layer gel film of lithium borate hydrate	18
Figure 12 Transformed gel single-layer to lithium tetraborate.....	19
Figure 13 Transformed gel multi-layer to lithium tetraborate	19
Figure 14 Devices fabricated on thick lithium tetraborate films	20
Figure 15 First electronic polymer detector for nuclear radiation	21
Figure 16 Concept for a polymer thermal neutron detector.....	22
Figure 17 Concept for a multi-layer polymer thermal neutron detector.....	22
APPENDIX A	23
DISTRIBUTION.....	24

Introduction

Neutron counters based on boron and lithium semiconductors have potential to expand the utility of neutron interrogation techniques for many security and nondestructive testing scenarios. Motivation for investigating semiconductor detectors includes improved efficiency, size, weight, ruggedness, reliability, timing, and spatial resolution made possible with solid-state detectors.

Current detector types have limited efficiencies. Efficiency is generalized:

$$(1) \quad \varepsilon = \xi(1 - e^{-N\sigma t}),$$

where ξ contains geometrical efficiencies, N is density, σ is neutron capture cross section and t is the thickness of medium converting neutrons to detectable particles. Gas media (BF_3 , ^3He) suffer from low N , requiring bulky, pressurized tubes to achieve sensitivity. Indirect detectors rely on converter foils, requiring small thickness to enable charged particles to escape into the detection medium. However, for direct semiconductor counters the conversion occurs within a condensed detection medium, resulting in N up to 1000 times higher than gas detectors. Since the secondary particles are generated within the active volume, conversion particle ranges do not limit thickness, enabling compact, high efficiency solid state detectors

Relative to scintillators, semiconductors offer potential advantages of stability, good signals characteristics and reliability. Solid-state ionization chambers have been developed for both gamma and charged particle radiation because of the large signal or 'gain' resulting from the creation process of electron-hole pairs in semiconductors. In scintillators, typically 50 eV or more of energy must be deposited into the crystal to produce a single optical photon, while only a few eV is necessary to create an electron-hole pair, thus a much greater signal is generated for a given amount of energy deposited. When signal losses associated with optical coupling and photodetector quantum efficiencies are considered in scintillator designs, semiconductor detectors become even more favorable. The reason that a solid-state design has not yet been developed for neutrons is that the conventional material choices (Si, Ge) are not thermal neutron sensitive. In general, semiconductor detectors have proven to be very versatile. They possess the high stopping efficiency of solids, an all-electrical and efficient manner of extracting signals, compact sizes, rugged operation, and in more advanced forms, position sensitive detection.

In designing a solid-state neutron detector, one would draw desired properties from amongst the existing gas, scintillator and semiconductor detectors. The scintillator has a high efficiency for stopping neutrons while the gas detector inherently has very low detection probabilities for gamma radiation. The simple operation and compactness of a semiconductor detector would be the biggest change in neutron detectors. Ease of distinguishing between neutron and gamma events would also be extremely beneficial. A large signal-to-noise ratio allows for simplified electronics and data acquisition.

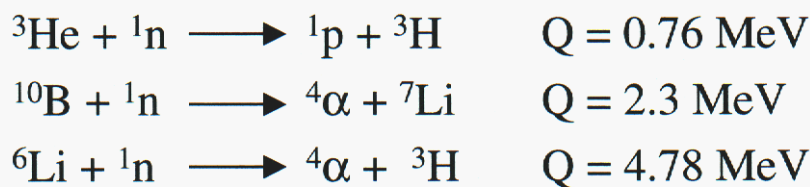
The material to construct such a detector should have the following material and electrical characteristics - 1) a composition that contains capture isotopes as constituent elements, 2) a relatively low effective atomic number, 3) a wide bandgap (> 1.5 eV) to insure low leakage currents at room temperature, 4) practical growth conditions, 5) a high conversion gain, 6) good charge transport to maximize signal size, and 7) ease of fabrication.

In this study a number of candidate materials have been ranked according to transport properties of currently available crystals. Resistivity and trapping time requirements for this application are considerably less demanding than for semiconductor gamma counters and spectrometers, because of the high Q for the conversion reactions with ^{10}B and ^6Li .

Experimental Details

Physics of detector operation

The conversion of thermal neutrons to energetic charged particles is effected by the reactions listed below. Of the roughly 2500 known isotopes, three practical stable species have the combination of high capture cross section and conversion to only charged particles. For solid-state detection, this limits our scope to solid materials with the isotopes ^6Li and ^{10}B as a major constituent. The cross sections for these isotopes are listed in Appendix A for convenience.



The ionized carriers are collected by application of an external electric field in a pulse photoconductive mode as a solid state ionization chamber.

Measurement circuit

The measurement circuit block diagram is shown in Figure 1. Samples under test are exposed to ionizing radiation in the form of alpha or neutrons, and the charge is measured via an Ortec 142 charge amplifier. Typically the pulse output is viewed and recorded on an oscilloscope, and may be routed through a shaping amp (Ortec 672) to a multichannel analyzer for recording a histogram. Typical data are shown above the diagram.

Results

Survey of candidate materials

A number of candidate materials were surveyed by Sandia in conjunction with Radiation Monitoring Devices of Watertown, MA. Material samples were metallized and exposed to ionizing radiation from isotopic or accelerator sources, and the relative response was evaluated. A partial tabulation of the results is given below:

Material	Results / Observations
Pyrolytic BN	Strong pulse response to alpha and neutron radiation. Severe polarization
Pure LiF, TLD600, TLD600H	All lithium fluoride based Crystalline samples showed similar α particle response in both polarities, indicative of active bulk Dopants plausible cause of different responses, suggests means for future improvement Successful neutron detection
α -BBO ($\text{Ba}_2\text{B}_4\text{O}_7$)	Best α particle response observed at Sandia High relative sensitivity measured via IBIC Successful neutron detection
Pure $\text{Li}_2\text{B}_4\text{O}_7$, TLD800	Largest S/N observed via α particle tests Strong neutron response Dopants are plausible cause of different responses
LiTaO_3	Good x-ray response Poor α particle response
LiGaO_2	Good x-ray response Poor/weak α particle response
LiAlO_2	Poor x-ray response Poor α particle response
LiNbO_3	Poor x-ray response Poor α particle response
LiInSe_2	Electrically unstable Some α particle response, difficult to measure Experimental, difficult to grow material

Investigation of pyrolytic BN

Hexagonal pBN has some excellent properties for a neutron sensitive detector, including a high concentration of absorbing nuclei and extremely high dielectric strength, and the low effective atomic number of BN makes it almost transparent to gamma rays. A thin detector is also beneficial to charge collection, making it easier to extract signals from materials with low carrier mobilities and lifetimes.

Properties of pBN

High σ (natural, pure ^{10}B)	767, 3835	barns
Low absorption lengths	226, 49	μm
High Q (94%, 6%)	2.3, 2.8	MeV
High spatial resolution	1.2	μm
Low Z (B, N)	10, 14	
High threshold dE/dx	> 14	eV/Angstrom

Samples of “turbostratic” microstructured material were provided by Advanced Ceramics, Cleveland Ohio, Figure 2. The density of Advanced Ceramics’ pBN ranges from 1.95 to 2.22 g/cm³, comparable to various hot pressed forms. The pBN samples lapped to 0.004”-0.005” thick were prepared. Small electrodes were then applied to form simple planar devices. The first irradiation tests were conducted with an isotopic ^{241}Am source. (^{241}Am produces 5.5 MeV alpha particles that are highly ionizing and have short penetration depth, thus providing a useful tool for studying thin detectors). The pBN devices were readout using standard nuclear pulse counting electronics and the resultant data was stored in a multichannel analyzer.

Shown in Figure 3 is a pulse height spectrum collected at 400 V bias. A clear pulse height distribution is seen above the noise occurring below approximately channel 40. As compared to the injected pulser peak at the high end of the spectrum (channel 240), the alpha particle induced distribution is far broader indicating that electronic noise is not a dominating factor. The width of the alpha peak distribution may be explainable through spatial nonuniformity of electrical properties or varied amounts of deposited energy (possibly as a function of interaction depth) within the pBN layer.

Further results were obtained versus applied detector bias. Experiments of this type are used to better understand the material’s charge collection properties and determine conversion values (E_{pair}). Figure 4 shows the progression of the pulse height distribution as bias increased on the detector from 25 to 150 volts. Both the number of counts within the distribution and its centroid increase. The increase in centroid position is expected, however the peak broadening and the increased number of counts are not typical for ohmic contact radiation detectors. This is further exemplified in Figure 5 which plots the

peak centroids versus bias and compares the curve shape with that from the Hecht model (the standard model for planar, Ohmic detectors). Experimental curves for both electrons and holes are shown and are obtained by selectively irradiating the cathode and anode, respectively. The apparent lack of agreement between the model and data suggests that the pBN devices are not behaving as Ohmic devices and are possibly not fully depleted.

The detectors were evaluated for neutron sensitivity at the McClellan Nuclear Radiation Center in Sacramento, CA. The devices were exposed to thermal neutrons and gamma flux from a TRIGA reactor designed for n radiography. Response proportional to reactor power was recorded, but the response to neutrons was found to diminish severely over short (30 minute) exposure to $1\text{E}6\text{ n/cm}^2/\text{s}$. This polarization effect was observed in all samples.

Investigation of Borate Crystals

Borates of lithium and barium were found to be good candidates in the initial screening of materials prior to this project. In fact, before this work began collaborations with Inrad Corporation and Radiation Monitoring Devices were initiated to investigate these materials grown from the melt, as opposed to the usual flux methods employed for optical crystals. It was found that charge collection in crystals grown from stoichiometric melts was considerably improved over flux-grown samples containing high sodium content. Figure 9 shows a neutron pulse height distribution taken in vacuum in Sandia's 3MeV tandem accelerator with a barium borate crystal detector made from Inrad's material. Approximately $1\text{E}8$ neutrons/s were generated by the threshold reaction with a thick lithium target. This result was subsequently corroborated by RMD in their laboratory using fission neutrons from a Californium source.

Hemry et al reported thick films of lithium tetraborate from aqueous gels.¹ Successful fabrication of neutron-sensitive bulk semiconducting films by a simple spin-casting approach could revolutionize neutron sensing and imaging, possibly enabling low cost, very large area detectors and arrays. Therefore synthesis of such films was investigated during this project.

The approach was to spin-cast the hydrated gel from solutions in the lithium oxide-boric oxide-water system. Following drying of the gel films at 280 C for 15 minutes, transformation to crystalline $\text{Li}_2\text{B}_4\text{O}_7$ by heat treatment at 500 C. Figure 10 is an optical micrograph of a single sub-micron layer of the dried gel. Thick deposits must be made by multiple spin-casting and baking steps. However, difficulties with re-hydration of the dried gel require heat treatment between coats, as seen in Figure 11. Poor morphology and delamination otherwise result. Multiple layers of gel in the micrograph shows typical swelling and wrinkle caused by re-hydration during second and subsequent spin-casting steps.

¹ J. D. Hemry, M. C. Weinberg, D. R. Uhlmann, "Lithium tetraborate gel films from aqueous solution, J. Mat. Sci. 33 (1998) 3853-8.

Successful transformation to smooth, dense films is easily achieved for single layers, as seen in the micrograph of Figure 12. The correct crystal structure was confirmed by XRD on multiple layer films. However, production of thicker films by building up multiple layers was difficult due to cracking of the thick deposit during transformation. Figure 13 shows a thick film built up through 8 spin-dry-bake cycles to a thickness of several microns. Cracking and blistering can be avoided by careful control of solution and spinning parameters.

Device structures were defined by gold e-beam evaporation through a shadow mask. Typical results are seen in the optical micrographs of Figure 14. Unfortunately, no neutron sensitive devices were achieved in this study.

Investigation of Polymer Composite Materials

During the course of this work, polymer materials under investigation for light emitting devices were made available for evaluation. Early results supported by this project indicated some of these films were sensitive to alpha particle radiation. The first result is shown in Figure 15. This result excited interest in polymer-based radiation detection, resulting in a host of new projects supported by various customers including LDRD and DOE NA22. However, only limited work was performed to evaluate polymers for use as thermal neutron detectors relevant to the goals of this project.

One means to use these materials for thermal neutron detection is to design a composite containing boron or lithium or nanoparticles to convert the neutrons. An attempt was made to incorporate boron nanoparticles into a poly paraphenylene vinylene (PPV) derivative, however the particles degraded the photoconductivity of the polymer, and no further compositions were produced.

Another approach is to make a bilayer structure of a boron loaded material in contact with the sensitive polymer. This idea is illustrated in Figure 16. This concept for a polymer based thermal neutron detector is the same as a traditional the converting foil but could be easier and cheaper to fabricate. The example shown assumes an interdigitated electrode structure to sense the charge.

Of course, single layer efficiency would be limited by range of ions in the converting foil. An extension of this idea is to laminate many bilayers together into a thick composite material, as illustrated in Figure 17. This design requires drifting the charge in the plane of the device, and deep damascene interdigital electrodes are assumed in the figure. Fabrication of similar structures (without the boron) has recently been demonstrated in an Exploratory Research project for NA22.

Summary and Conclusion

In the course of this work bulk samples of lithium tetraborate and pyrolytic boron nitride from commercial vendors were used to demonstrate solid state detection of thermal neutrons. Good progress has been made toward each of the research goals of this project. Difficulties with pBN including poor reproducibility and count rate polarization were noted. Therefore LBO received more attention for the latter part of the project.

US patent 6,388,260 was granted to Sandia during this work, on the use of lithium tetraborate for neutron detection. Bulk crystal counters were first demonstrated previously by Sandia using commercial LBO, and in-house synthesis of LBO films by a spin-on gel casting was investigated as a potential low cost production method. The gel-cast films have high resistivity and appear stable under high electric fields. However, none of the films made to date have been sensitive to radiation.

Bulk LBO devices were fabricated and tested using a proton beam to evaluate charge collection properties. The estimated mobility-lifetime products for bulk LBO from this analysis are on the order of $1\text{E}-10\text{ cm}^2/\text{volt}$. Based on these results, the performance expected from LBO pixels with an existing readout chip (developed by Oak Ridge for a high-energy physics application) was quantitatively determined. The model evaluates leakage current, capacitance and charge collection efficiency versus pixel geometry and bias. Signal to noise ratios in the range of 2 to 20 are predicted for 256 to 32 micron spatial resolution arrays.

A result of this project was new work to evaluate the feasibility of organic semiconductors for radiation detection. Films apparently sensitive to alpha radiation were tested, and this data excited interest in several new research projects. An attempt to make a thermal neutron sensitive composite by loading a PPV derivative with boron nanoparticles resulted in degradation of the photoconductivity. Approaches to laminar composites were designed for future work.

Measurement Circuit

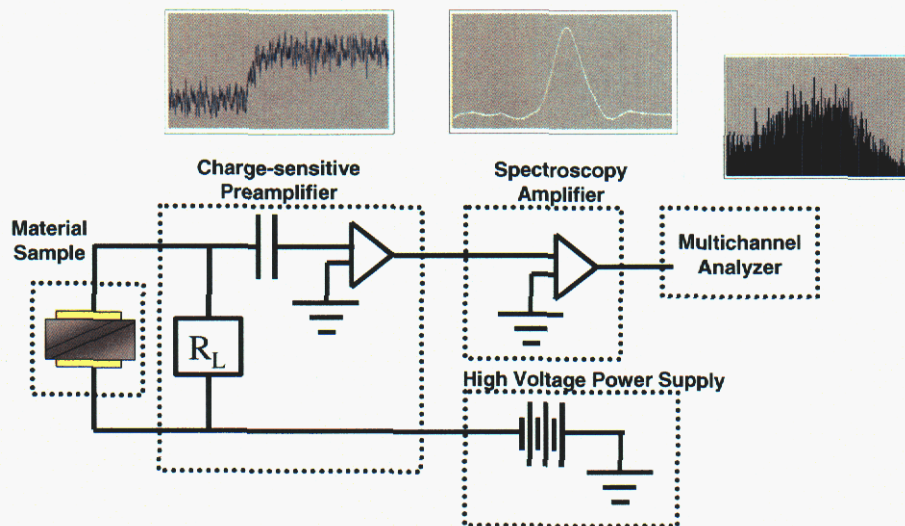


Figure 1. Measurement circuit block diagram. Ortec 142 A CSA and 672 shaping amplifier were used to measure charge collection and pulse height distributions.

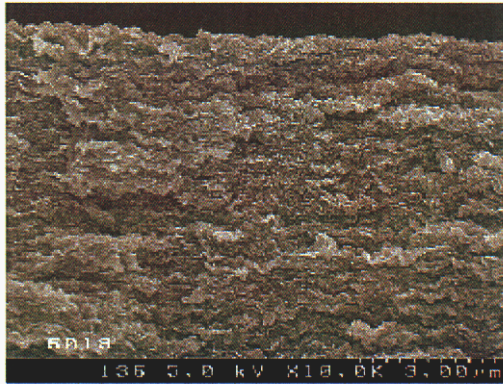


Figure 2. An SEM micrograph of a pBN layer showing strong twinning. The crystallographic 'c' axis is oriented vertically. The entire field of view is approximately 10 μm wide, as denoted by the 3 μm bar in the lower right. Courtesy of Advanced Ceramics.

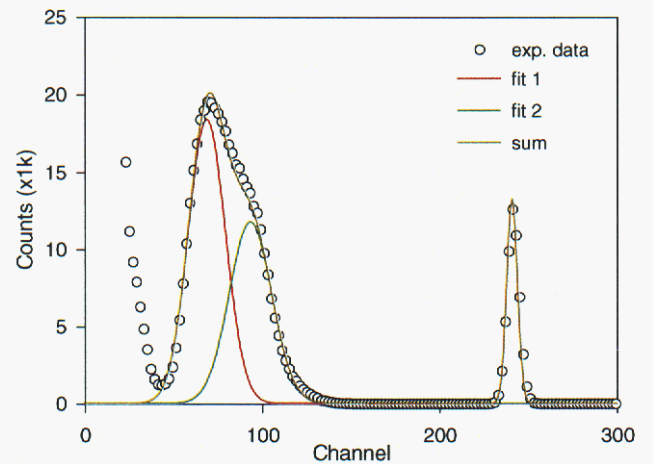


Figure 3. Response of pBN device to ^{241}Am alpha particle irradiation. Spectrum collected at 400 V and shaping time constant of 10 μs . The alpha particle response is well matched to a pair of Gaussian distributions. At approximately channel 240, a pulser input indicates the electronic noise contribution to peak broadening.

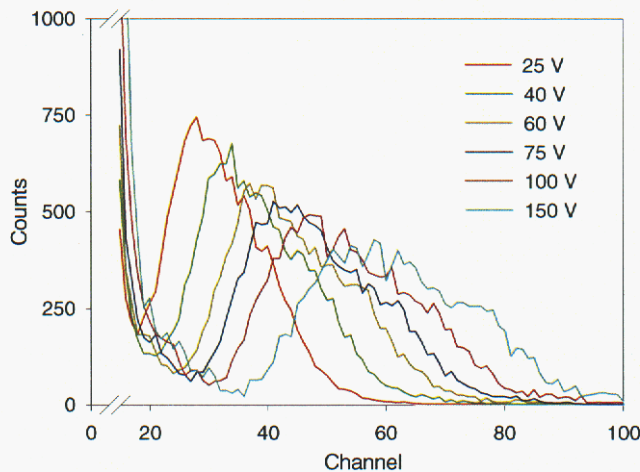


Figure 4. Bias dependence of pBN detector response to ^{241}Am alpha particles. Centroid or distribution (above noise threshold) and number of counts in distribution both increase with voltage.

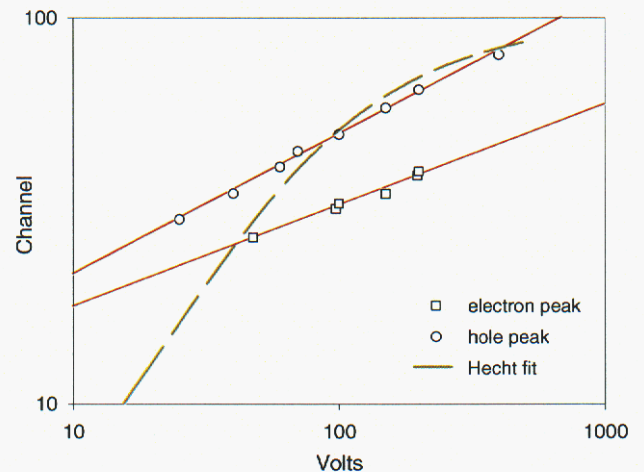


Figure 5. Distribution centroids versus detector bias from the alpha particle data. Separate data is given for electron and hole transport. The data follow linear power curves better than a theoretical Hecht fit. This suggests that the electric field in the pBN device is not uniform.

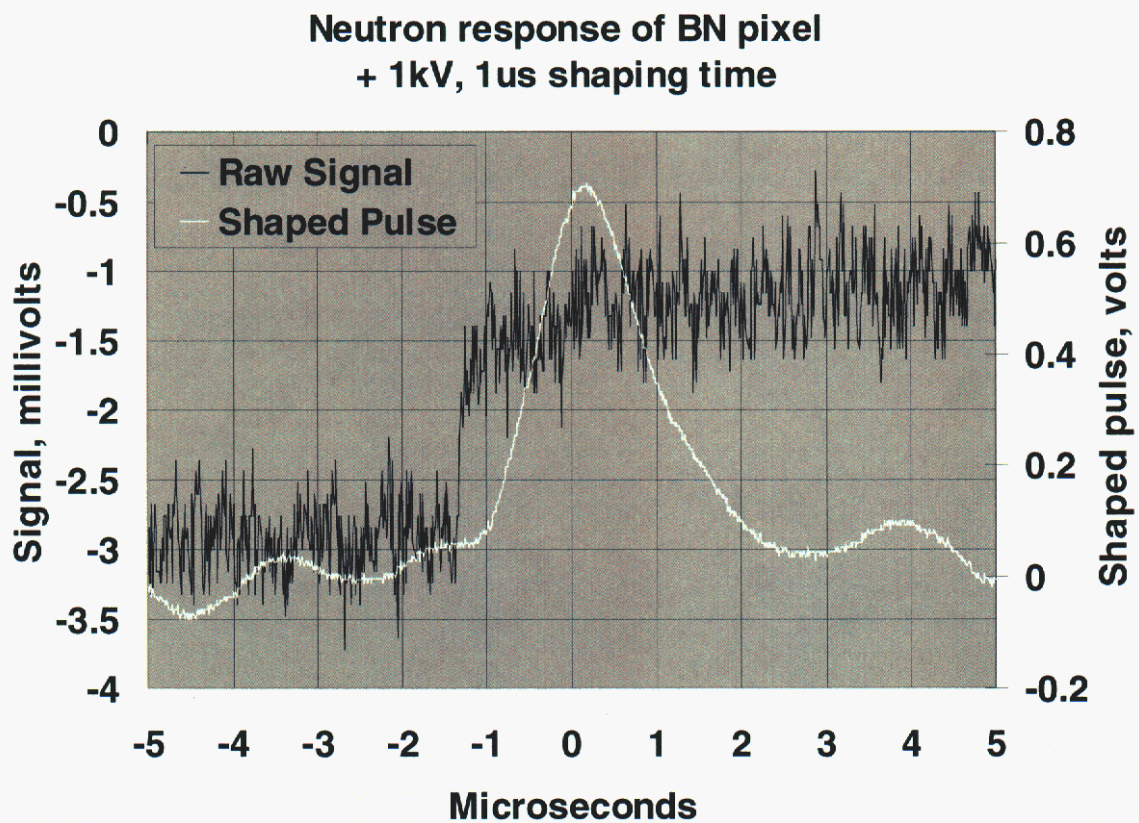


Figure 6. Pulse response of pBN to thermal neutrons from MNRC TRIGA reactor.

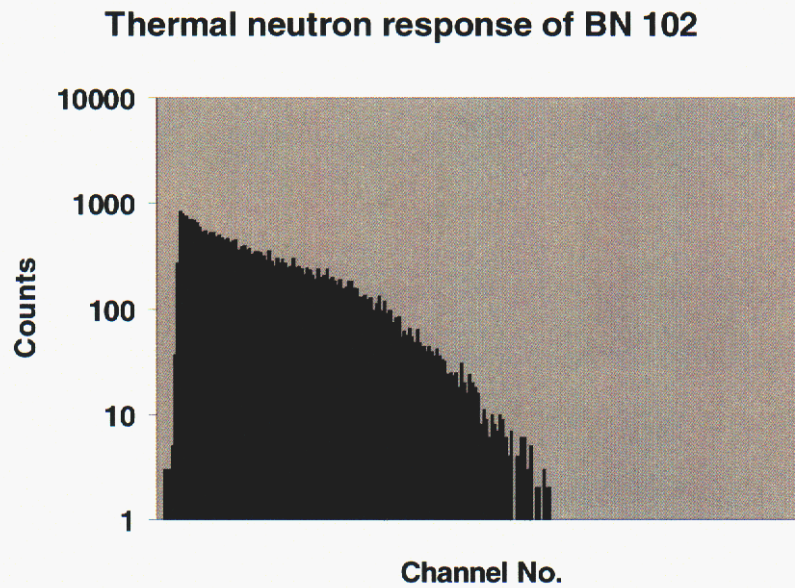


Figure 7. Pulse height distributions for thermal neutrons in pBN.

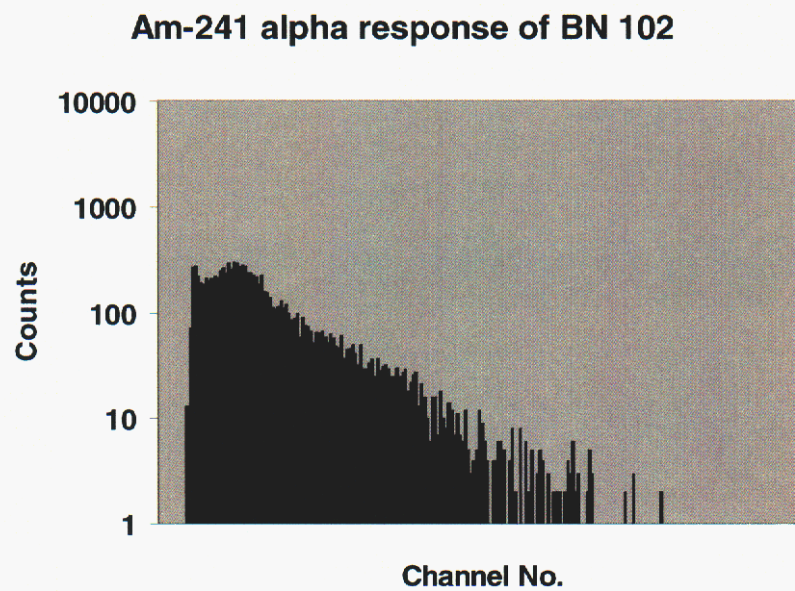


Figure 8. Pulse height distribution for isotopic alphas in pBN.

**Response of α BBO to radiation produced by 3MeV protons
on lithium gallate target. Shaping time 10 μ s.**

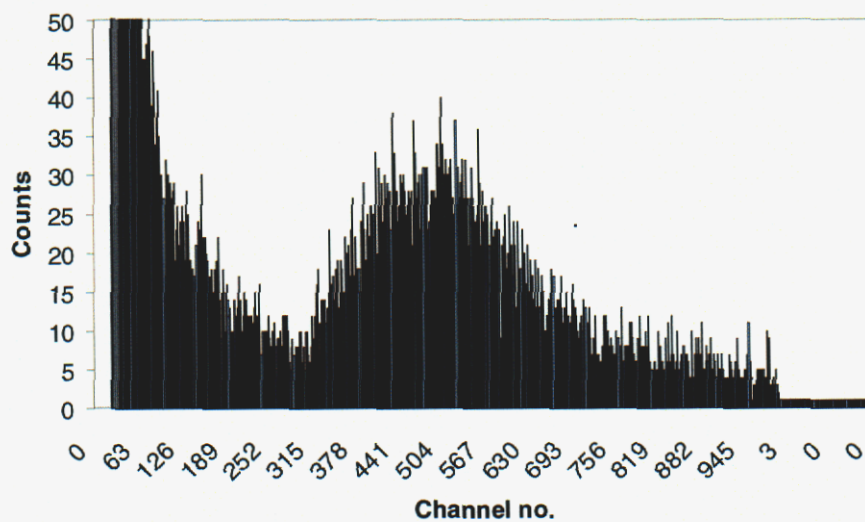


Figure 9. Response of barium borate to neutrons produced by 3MeV protons on a thick lithium target.

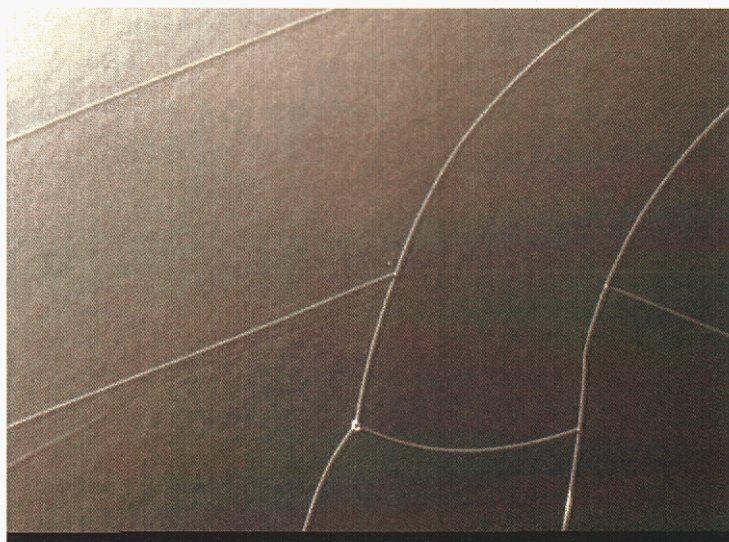


Figure 10. Single-layer gel film of lithium borate hydrate. Cracking typically for fast drying in 150 C oven. FOV 200 microns.

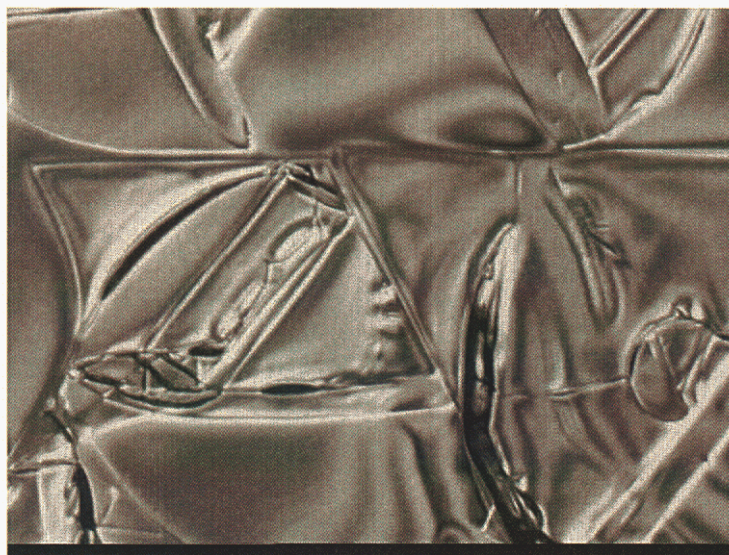


Figure 11. Thicker lithium borate hydrate gel films proved difficult to cast. Multiple layers of gel in micrograph shows typical swelling and wrinkle caused by re-solvation during second spin-casting step. FOV 200 microns.

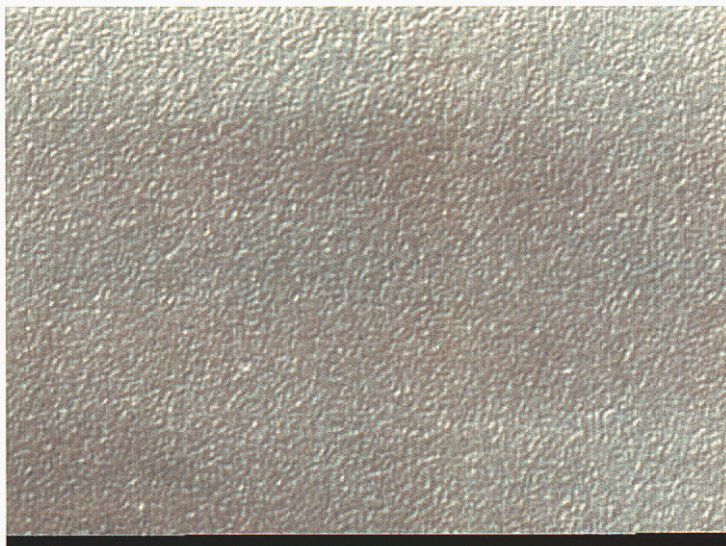


Figure 12. Smooth films of were easily obtained by 400 C bake of single gel-cast layers. The lithium tetraborate structure was confirmed by XRD. Image field of view 200 microns, film thickness < 1 micron. FOV 200 microns.

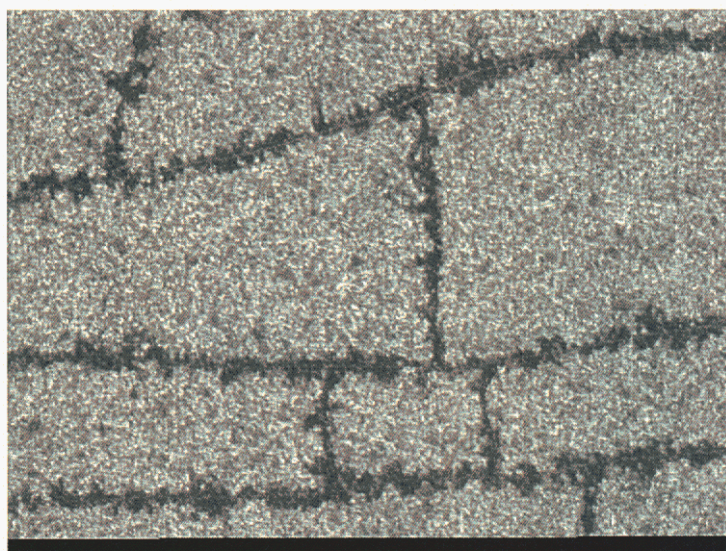


Figure 13. Production of thicker films by building up multiple layers was difficult due to cracking of the thick deposit during transformation. FOV 200 microns.

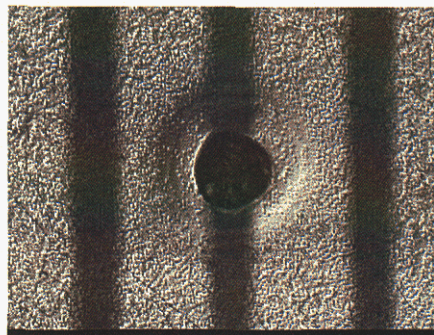
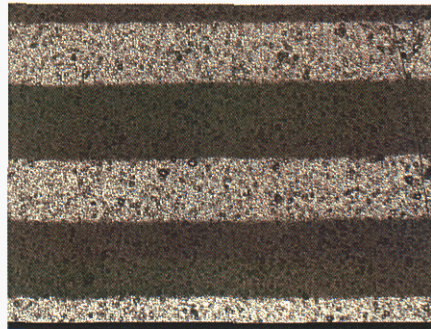
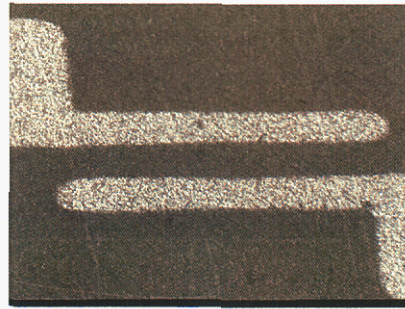


Figure 14. Detector arrays were defined by shadow-mask deposition of gold contacts. No neutron-sensitive films were achieved during this study. FOV 200 microns.

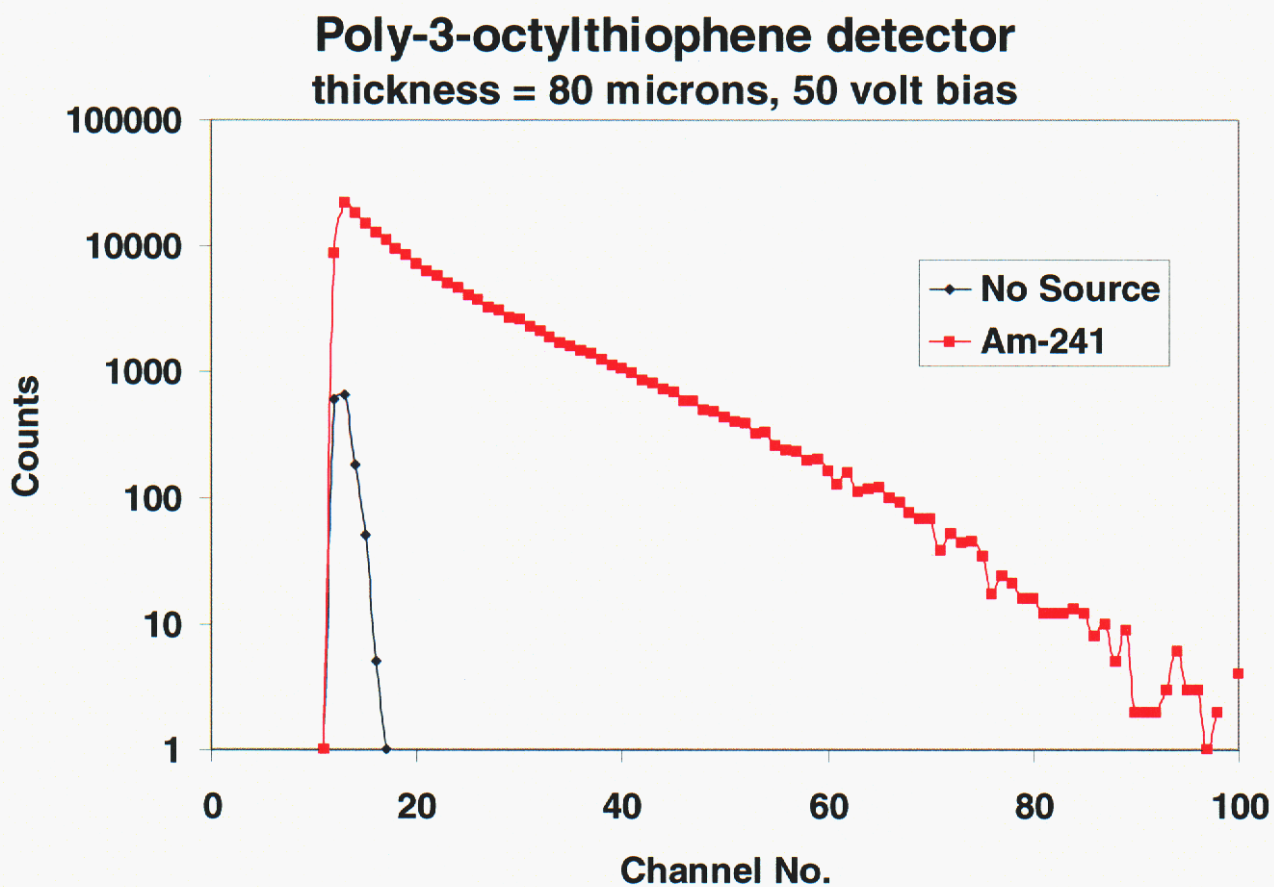


Figure 15. First electronic polymer detector for nuclear radiation.

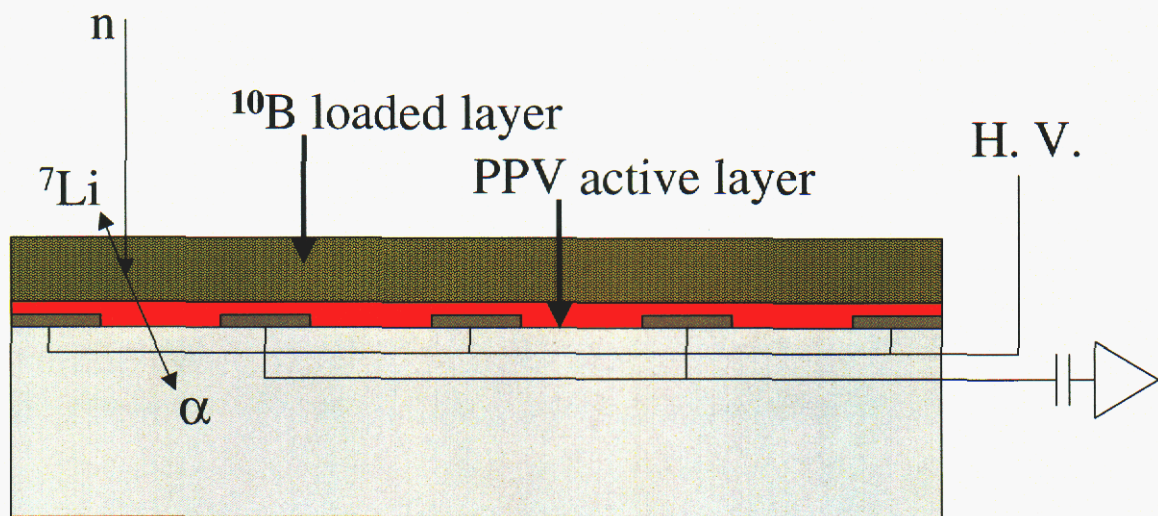


Figure 16. Concept for a polymer based thermal neutron detector. This design based on the converting foil approach could be easy to fabricate and inexpensive relative to traditional semiconductors. Single layer efficiency would be limited by range of ions in the foil.

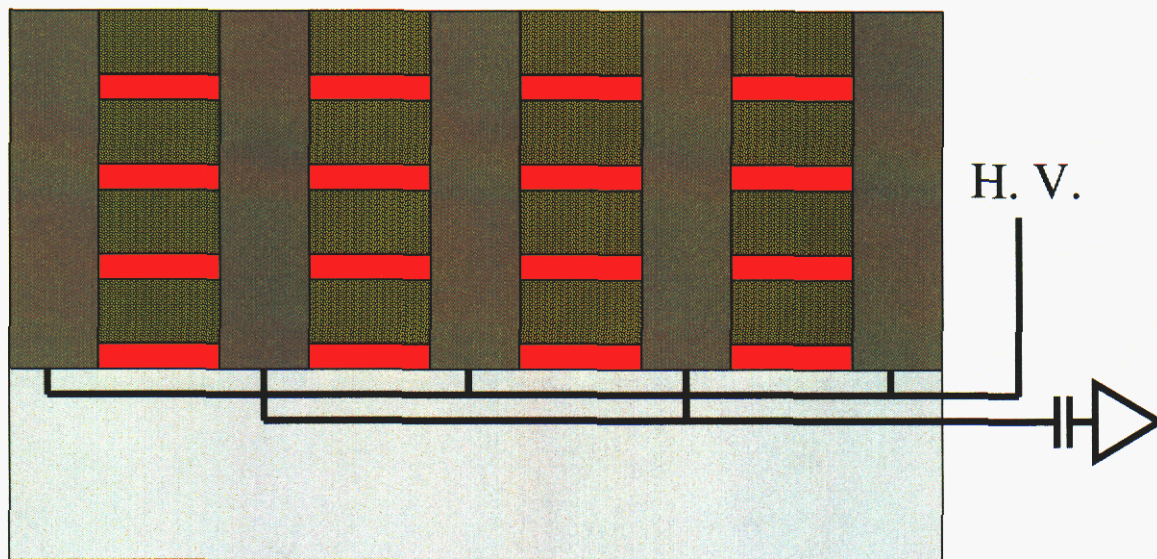


Figure 17. The efficiency could be increased by use of multiple layers.

Appendix A : Neutron cross sections for principal conversion isotopes

2-He- 3

REACTION	2200-m/s (barns)	Maxw.Avg. (barns)	Res.Integ (barns)	14-MeV (barns)	Fiss.Avg. (barns)
total	5.331 +3	4.743 +3		1.168	2.941
elastic	3.135	3.135		954.4 -3	2.121
nonelastic	5.328 +3	4.722 +3	2.381 +3	213.8 -3	819.6 -3
capture	54.01 -6	47.88 -6	246.9 -6	35.18 -6	39.24 -6
(n,p)	5.328 +3	4.722 +3	2.381 +3	139.7 -3	816.9 -3
(n,d)		(E-thr = 4.362 MeV)		74.07 -3	2.647 -3
30-keV Maxwellian spectrum average neutron capture = 1.255E-02 millibarn					

3-Li- 6

REACTION	2200-m/s (barns)	Maxw.Avg. (barns)	Res.Integ (barns)	14-MeV (barns)	Fiss.Avg. (barns)
total	941.1	837.2		1.431	1.900
elastic	734.5 -3	735.2 -3		906.4 -3	1.422
nonelastic	940.4	836.5	427.5	525.0 -3	478.0 -3
inelastic		(E-thr = 1.751 MeV)		412.0 -3	142.8 -3
(n,2n)		(E-thr = 6.614 MeV)		78.05 -3	190.5 -6
capture	38.50 -3	34.11 -3	17.47 -3	82.11 -6	28.06 -6
(n,p)		(E-thr = 3.185 MeV)		6.766 -3	4.264 -3
(n,t)	940.3	833.4	424.9	28.04 -3	330.7 -3
30-keV Maxwellian spectrum average neutron capture = 4.503E-02 millibarn					

5-B - 10

REACTION	2200-m/s (barns)	Maxw.Avg. (barns)	Res.Integ (barns)	14-MeV (barns)	Fiss.Avg. (barns)
total	3.840 +3	3.415 +3		1.467	2.638
elastic	2.144	2.144		942.5 -3	2.062
nonelastic	3.838 +3	3.413 +3	1.726 +3	524.2 -3	575.3 -3
inelastic		(E-thr = 0.791 MeV)		268.5 -3	70.84 -3
(n,2n)		(E-thr = 8.980 MeV)		26.83 -3	33.22 -6
capture	500.0 -3	443.1 -3	224.9 -3	21.26 -6	76.03 -6
(n,p)	3.000 -3	2.659 -3	94.96 -3	37.51 -3	15.25 -3
(n,d)		(E-thr = 4.801 MeV)		47.63 -3	1.249 -3
(n,a)	3.837 +3	3.400 +3	1.719 +3	48.95 -3	435.5 -3
(n,t2a)	12.00 -3	10.63 -3	305.2 -3	94.66 -3	52.28 -3
30-keV Maxwellian spectrum average neutron capture = 5.828E-01 millibarn					

Distribution

1	MS 0323	D. Chavez, LDRD Office, 1011
1	MS 9001	John, M.E. – 8000 Attn: Stulen, R.H. – 8100, MS 9004 Henson, D.R. - 8200, MS 9007 McLean, W.J. - 8300, MS 9054 Smith, P.N. - 8500, MS 9002 Washington, K.E. - 8900, MS 9003
1	MS 9401	Talin, Albert Alec - 08751
1	MS 9402	Anderson, David W – 08772
1	MS 9402	Antolak, Arlyn – 08773
1	MS 9402	Balch, Dorian – 08772
1	MS 9402	Bastasz, Robert J – 08772
1	MS 9402	Brooks, John – 08772
1	MS 9402	Buchenauer, Dean – 08772
1	MS 9402	Cadden, Charles – 08772
1	MS 9402	Causey, Rion – 08772
1	MS 9402	Cowgill, Don – 08772
1	MS 9402	Doty, Patrick – 08772
1	MS 9402	Hertz, Kristin – 08772
1	MS 9402	Meeker, Don – 08772
1	MS 9402	Odegard, Ben – 08772
1	MS 9402	Olsen, Richard – 08772
1	MS 9402	San Marchi, Christopher – 08772
1	MS 9402	Smugereksey, John – 08772
1	MS 9402	Somerday, Brian – 08772
1	MS 9402	Soo, Greg – 08772
1	MS 9402	Whaley, Josh - 08772
1	MS 9402	Wilson, Ken - 08770 Attn: Bill Replogle, 08771 Jim Wang, 08773 Paul Spence, 08774
3	MS 9018	Central Technical Files - 8945-1
1	MS 0899	Technical Library - 9616
1	MS 9021	Classification Office, 8511, for Technical Library, MS 0899, 9616 DOE/OSTI via URL
1	MS 0161	Patent and Licensing Office, 11500